Remote Sensing of Environment 247 (2020) 111916

Contents lists available at ScienceDirect

Remote Sensing of Environment

journal homepage: www.elsevier.com/locate/rse

Quantifying expansion and removal of *Spartina alterniflora* on Chongming island, China, using time series Landsat images during 1995–2018

Xi Zhang[a], Xiangming Xiao[b,*], Xinxin Wang[a], Xiao Xu[a], Bangqian Chen[c], Jie Wang[b], Jun Ma[a], Bin Zhao[a], Bo Li[a,**]

[a] Ministry of Education Key Laboratory of Biodiversity Science and Ecological Engineering, Coastal Ecosystems Research Station of the Yangtze River Estuary, Institute of Biodiversity Science, School of Life Sciences, Fudan University, Shanghai 200438, China
[b] Department of Microbiology and Plant Biology, University of Oklahoma, Norman, OK 73019, USA
[c] Rubber Research Institute (RRI), Chinese Academy of Tropical Agricultural Sciences (CATAS), Hainan Province 571737, China

ARTICLE INFO

Keywords:
Spartina alterniflora
Phenology
Time series Landsat images
Chongming island

ABSTRACT

The rampant encroachment of *Spartina alterniflora* into coastal wetlands of China over the past decades has adversely affected both coastal ecosystems and socio-economic systems. However, there are no annual or multi-year epoch maps of *Spartina* saltmarsh in China, which hinders our understanding and management of *Spartina* invasion. In this study, we selected Chongming island, China, where *Spartina* saltmarsh had expanded rapidly since its introduction in the 1990s. We investigated phenology of *Spartina*, *Phragmites* and *Scirpus* saltmarshes, and the time series vegetation indices derived from Landsat images showed that *Spartina* saltmarsh did not green-up in April–May and stayed green in December–January, which differed from the phenology of *Phragmites* and *Scirpus* saltmarshes. We developed a pixel- and phenology-based algorithm that used time series Landsat data to identify and map *Spartina* saltmarsh, and we applied it to quantify the temporal dynamics (expansion and removal) of *Spartina* saltmarsh on Chongming island during 1995–2018. The resultant maps showed that *Spartina* saltmarsh area on Chongming island increased from ~4 ha in 1995 to ~2067 ha in 2012 but dropped substantially to ~729 ha in 2016 after a large-scale ecological engineering project (US$ 186 million) was started to remove *Spartina* during 2013–2016. Chongming island still had ~1315 ha *Spartina* saltmarsh in 2018, and majority of it was distributed outside the Chongming Dongtan National Nature Reserve, which could serve as the sources for reinvasion in the near future. This study demonstrates the feasibility of using time series Landsat images, pixel- and phenology-based algorithm, and GEE platform to identify and map *Spartina* saltmarsh over years in the region, which is useful to the management of invasive plants in coastal wetlands.

1. Introduction

Biological invasion has been one of the most crucial ecological issues in the coastal wetlands worldwide (Mao et al., 2019; Vaz et al., 2018). *Spartina alterniflora* (hereafter, *Spartina*), a C_4 grass growing primarily in the Atlantic coastal regions of North America, was first introduced to China in December 1979 (Zuo et al., 2012). The original purpose of *Spartina* introduction to China was for soil amelioration, tidal reclamation and erosion mitigation (Li et al., 2009; Lu and Zhang, 2013; Xiao et al., 2010). However, with its high survivability and strong adaptability, introduced *Spartina* has been well established in the intertidal zones and become a dominant species in saltmarshes in China (Wan et al., 2014). As time passed, the overwhelming spread of *Spartina* populations threatened the coastal environments by altering the estuarine sediment dynamics, outcompeting native plant species, and reducing bird biodiversity due to losses of food resources and feeding habitats. China has the largest area of exotic *Spartina* (Liu et al., 2018). In 2003, *Spartina* was listed as one of the most harmful invasive plants by the Ministry of Environmental Protection of China (Chung, 2006). Accurate, consistent, and comprehensive records of *Spartina* saltmarsh in China are urgently needed for ecological management and coastal ecosystem conservation. However, to date, no datasets of *Spartina* saltmarsh at high spatial resolution and annual temporal resolution in China are available to the stakeholders and public.

* Corresponding author at: Department of Microbiology and Plant Biology, University of Oklahoma, Norman, OK 73019, USA.
** Corresponding author at: Ministry of Education Key Laboratory of Biodiversity Science and Ecological Engineering, Institute of Biodiversity Science, Fudan University, Shanghai 200433, China.
E-mail addresses: xiangming.xiao@ou.edu (X. Xiao), bool@fudan.edu.cn (B. Li).

https://doi.org/10.1016/j.rse.2020.111916
Received 3 November 2019; Received in revised form 20 May 2020; Accepted 24 May 2020

Table 1
A brief summary on image data sources and methods used in previous studies for classifying and mapping *Spartina* saltmarsh.

Methods		Multi-spectral images		Hyperspectral images	Multi-source images
		VHSR	HSR		
Visual interpretation Images and spatial statistics of images	MLC	Liu et al. (2017)	Zhang et al. (2004); Wan et al. (2014)		
		Liu et al. (2016); Ai et al. (2017)	Li et al. (2006); Huang and Zhang (2007b); Lu and Zhang (2013); Zhang et al. (2017)		Chust et al. (2008); Hladik et al. (2013)
	NN	Morris et al. (2005)			
	SVM	Ai et al. (2017)	Wang et al. (2015); Liu et al. (2018); Mao et al. (2019)		
	RB/DT/RF	Wan et al. (2014); Lin et al. (2015); Wang et al. (2015)	Zuo et al. (2012); Sun et al. (2016)		Hladik et al. (2013); van Beijma et al. (2014)
	SMA		Zhu et al. (2016)	Rosso et al. (2005)	
Pixels and temporal statistics of pixels			**This study**		

Note: **VHSR**: Very high spatial resolution satellite image (e.g., GF-1); **HSR**: high spatial resolution satellite image (e.g., Landsat); **MLC**: Maximum likelihood classification; **NN**: Artificial Neural Network; **SVM**: Support vector machine; **RB**: Rule-based; **DT**: Decision tree; **RF**: Random forest; **SMA**: Spectral mixture analysis.

Remote sensing is an effective tool for ecological monitoring and management of invasive plants (Bradley, 2014; Wang et al., 2017). Image data from satellite and airborne sensors, coupled with geographic information systems (GIS) and advanced cloud computing system, offer researchers viable tools to detect and monitor the distribution of invasive plants. Table 1 provides a brief summary on *Spartina* saltmarsh classification and mapping over the past two decades. One approach is to carry out visual interpretation and digitalization of single or multi-date images and generate *Spartina* saltmarsh maps (Liu et al., 2017; Wan et al., 2014; Zhang et al., 2004). This approach is labor-intensive and time-consuming, and the resultant maps often have large uncertainty when images from different acquisition dates are used or interpreted by different researchers. The second approach is to use single or multi-date hyperspectral or multi-spectral optical images, calculate the spatial statistics of spectral bands, vegetation indices and texture in these images, and apply supervised or unsupervised classification algorithms (e.g., maximum likelihood, random forest, support vector machine) to generate *Spartina* saltmarsh maps (Liu et al., 2016; Lu and Zhang, 2013; Mao et al., 2019). Many studies used Landsat images (Liu et al., 2018; Zhang et al., 2017) and selected one to multiple images based on image quality and other factors (e.g., tidal level). Because of large tidal dynamics and many human activities, the resultant maps of *Spartina* saltmarsh from the analyses of single or multi-date images in a year also have large uncertainty. To date, most of previous studies generated *Spartina* saltmarsh maps at either specific year(s) or small study region(s). The third approach is to use time series data of individual pixels, calculate the temporal statistics of spectral bands and vegetation indices in the pixels, and apply decision trees or rule-based algorithms to generate annual maps of *Spartina* saltmarsh. Phenological differences of plant species, which are documented in the time series data of spectral bands and vegetation indices, are carefully studied and the unique phenological features are identified, selected and used for classification of individual pixels. In recent years, the pixel- and phenology-based algorithms have been used in a number of studies for crops, tree plantations, coastal tidal flats and coastal vegetation (Dong et al., 2016; Helman et al., 2015; Kou et al., 2015; Wang et al., 2018).

Gao and Zhang (2006) and Ouyang et al. (2013) conducted *in-situ* field studies to collect hyperspectral data of coastal saltmarshes on Chongming island, Shanghai, China over different seasons and they found that *Spartina* has unique spectral characteristics that are different from other native saltmarsh plants in spring and fall seasons. In all multi-spectral bands and vegetation indices, Normalized Difference Vegetation Index (NDVI) in the senescence stage was considered to be useful for identifying *Spartina* saltmarsh (Ouyang et al., 2013). The phenological information of coastal saltmarshes acquired from field studies provide valuable reference but is hardly to be used at large spatial scale. There are also some studies that used monthly NDVI data from the China GaoFen-1 satellite and China Huanjing-1 satellite to identify and map coastal saltmarshes (Ai et al., 2017; Sun et al., 2016), and NDVI in the senescence stage (November to mid-December) and the green-up stage (late April–May) was recognized as an useful indicator for identifying *Spartina* saltmarsh (Ai et al., 2017). Although these efforts have presented the significance of unique phenological stages for identifying *Spartina* saltmarsh, the developed methods faced challenges in the extension of the resulting classifiers and parameters and the high cost of commercial satellite images. Landsat imagery at 30-m spatial resolution over the period of 1984-present (Wulder et al., 2019; Wulder et al., 2016) is an undoubtedly suitable data source for mapping long-term dynamics of *Spartina* saltmarsh. One pilot study evaluated the potential of time series Landsat images in 1984–2015 to track *Spartina* saltmarsh dynamics within the three pixels (500-m spatial resolution) of the Moderate Resolution imaging Spectroradiometer (MODIS) in the Yancheng Coastal Wetland Nature Reserve, Jiangsu province, China (Wu et al., 2018). However, the potential of time series Landsat images in tracking the phenological differences between *Spartina* and other native saltmarsh plants has not been fully assessed. Documenting the long-term and large-scale dynamics of *Spartina* saltmarsh would need to process a large volume of satellite images, which requires advanced and efficient computer

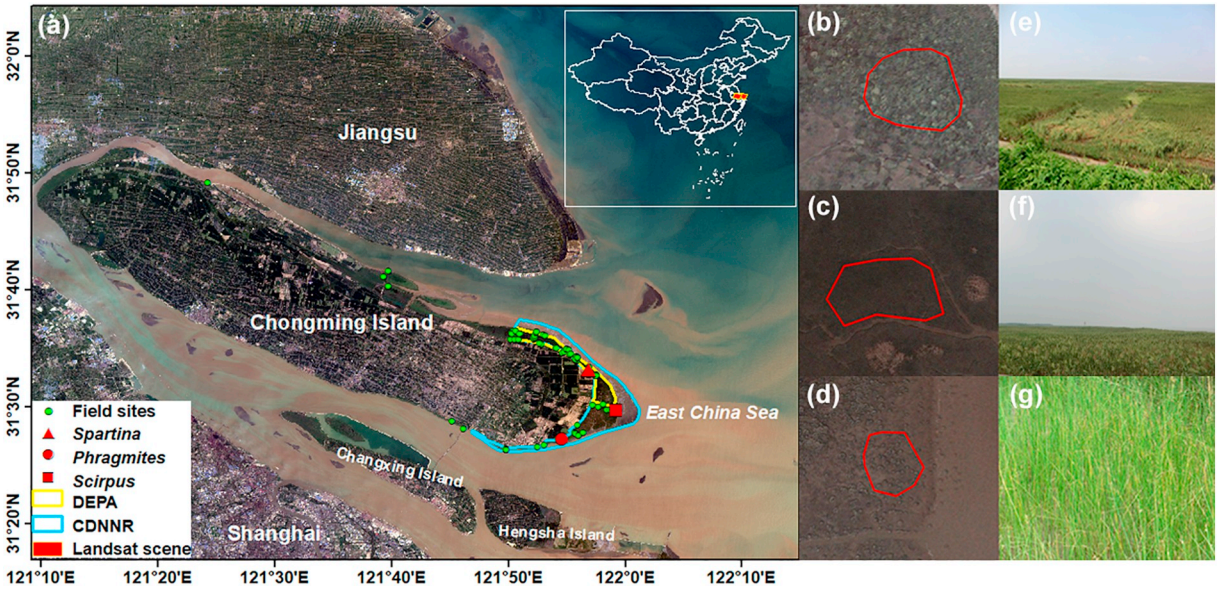

Fig. 1. The location of the Chongming island, Shanghai, China. It is within Landsat scene (path/row 118/38 and 119/38). (a) The locations of three field sites for *Spartina* (121.9481°, 31.5523°), *Phragmites* (121.9101°, 31.4531°) and *Scirpus* (121.9863°, 31.4932°) are shown, which were used for spectral signature analysis; (b, c, d) zoom-in view of landscapes from a very high spatial resolution image in the Google Earth (dated as 2012/11/01); and (e, f, g) field photos taken in August 2015 at the three field sites.

processing power. To develop a mapping tool that uses time series Landsat images, a pixel- and phenology-based algorithm, and the Google Earth Engine cloud computing platform to quantify and monitor the dynamics of *Spartina* saltmarsh over years would certainly address such needs.

In this study, we addressed the following questions: (1) what are the phenological differences between *Spartina* and other native saltmarsh plants as observed by time series Landsat images? (2) Do the time series Landsat images suffice to track phenology of *Spartina* and other native saltmarsh plants over years? (3) Is the phenology-based mapping algorithm with time series Landsat images reliable to discriminate *Spartina* saltmarsh from native saltmarshes? As a pilot and methodological study, we selected the Chongming island in the Yangtze River estuary, Shanghai, China, as case study area, which is the largest alluvial island in the world and has experienced both expansion and removal of *Spartina* in recent decades. The specific objectives of this study are: (1) to better understand the phenological characteristics of *Spartina* and other native saltmarsh plants on Chongming island with time series Landsat images; (2) to develop and evaluate a pixel- and phenology-based algorithm that uses time series Landsat images to effectively discriminate *Spartina* saltmarsh from other saltmarshes; and (3) to quantify the spatial-temporal dynamics of *Spartina* saltmarsh on Chongming island since the 1990s, which could illustrate the expansion dynamics of *Spartina* saltmarsh from the 1990s to 2000s and assess the effectiveness of the ecological restoration project to control and remove *Spartina* in the 2010s. The resultant maps of *Spartina* saltmarsh on Chongming island could be used to support conservation efforts and decision-making in Shanghai and the Yangtze River estuary. The resultant mapping tools could also be readily applied (and modified if needed) to identify and map *Spartina* saltmarsh in other coastal wetlands in China.

2. Materials and methods

2.1. Study area

Chongming island is part of the megacity Shanghai, China (31°27′-31°5 l'N, 121°09′-121°54′E), and is located at the mouth of Yangtze River (Fig. 1). It is the largest alluvial island in the world and covers an area of about 1267 km^2. It has a typical subtropical monsoon climate with an annual mean temperature of about 15.3 °C and annual mean precipitation of about 1022 mm. The eastern fringe of Chongming island is the Chongming Dongtan National Nature Reserve (hereafter, CDNNR), one of the largest nature reserves for migratory birds in Eastern Asia (Hu et al., 2015). The CDNNR was listed in the Chinese Protected Wetlands report in 1992, recognized as the Wetland of International Importance under the Ramsar Wetlands Convention in 2001, and designated as a National Nature Reserve for migratory bird conservation in 2005 (Xiao et al., 2010). The total area of the CDNNR is about 242 km^2, accounting for 20% of Chongming island area.

The commonest native plants in the study area are *Phragmites australis* (hereafter, *Phragmites*), *Scripus mariqueter* (hereafter, *Scirpus*) (Sun et al., 1992). In 1995, *Spartina* was first spotted in the north of the CDNNR. In an effort to reclaim more land for regional development by accelerating siltation, *Spartina* was intentionally planted in the CDNNR in 2001 (337 ha) and 2003 (542 ha), respectively (Wang, 2011). In 2007, the area of *Spartina* saltmarsh in Shanghai ranked third among all *Spartina*-invaded megacities and provinces in China, and the area of *Spartina* saltmarsh in Shanghai, Jiangsu, Zhejiang and Fujian accounted for 94% of the total area in China (Zuo et al., 2012).

In order to avoid the adverse effects of *Spartina* encroachment, Shanghai government had invested about ¥1.3 billion Chinese Yuan (US$ 186 million) to carry out an ecological restoration project (hereafter, DEPA) in the CDNNR since 2013 (Fig. 1a). The project had three major components: ecological eradiation of *Spartina*, restoration of native saltmarsh plant communities, and reconstruction of bird habitats (Tang, 2016). Its preliminary work was started in December 2010 and various technical methods were tested and evaluated during 2011–2012 in one demonstration area (~4 km^2). Large-scale restoration work was launched in December 2013, covering a total area of 24.19 km^2. The project region was enclosed with artificial levee for eradicating *Spartina* through cutting the plants and flooding the marshes (Hu et al., 2015).

2.2. Data

In this study we used time series Landsat datasets, images from Google Earth, and in-situ data to identify and map *Spartina* saltmarsh on Chongming island, and Fig. 2 shows the dataflow and workflow for image processing and classification.

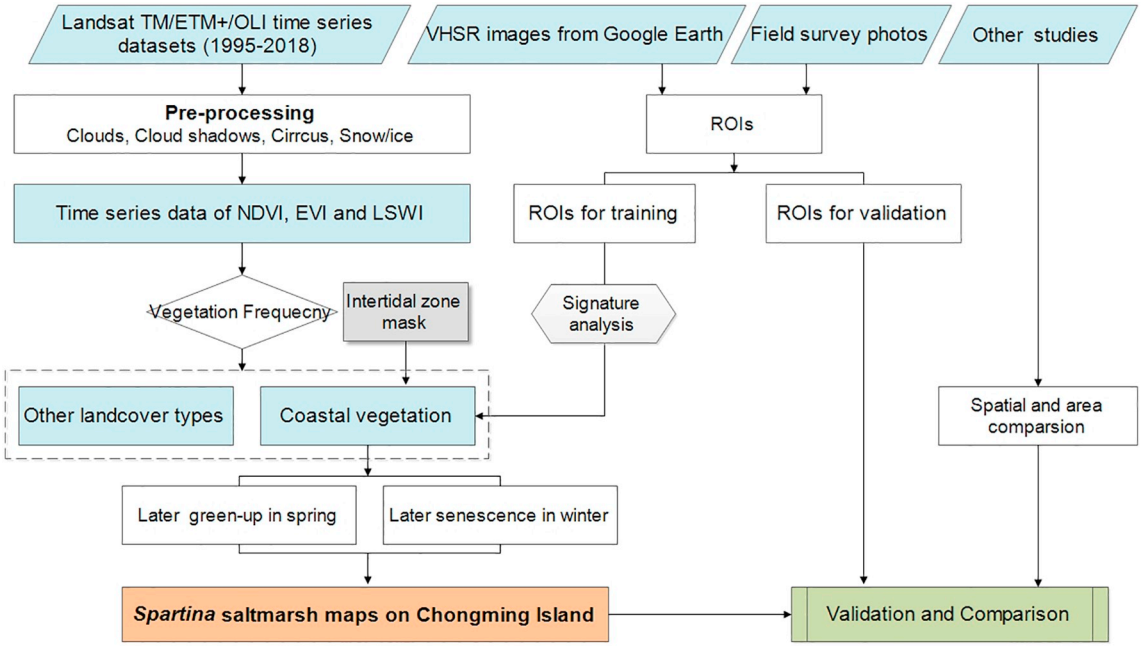

Fig. 2. The workflow for the pixel- and phenology-based *Spartina* saltmarsh mapping in this study.

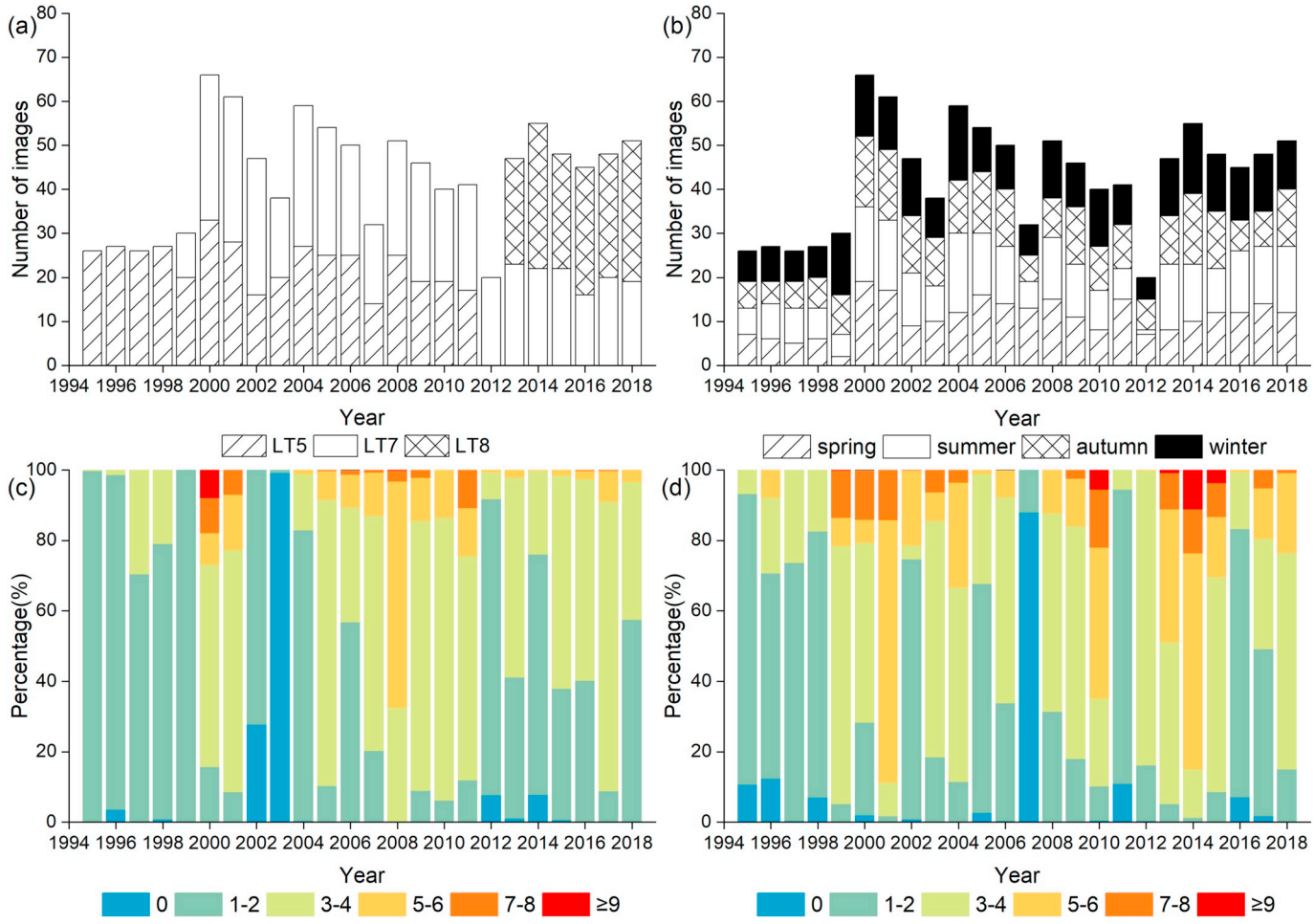

Fig. 3. The annual distributions of number of Landsat images (a) by sensors (Landsat5 TM, Landsat7 ETM+, and Landsat8 OLI), (b) by seasons (spring, summer, autumn, and winter), and percentage of pixels with various numbers of good-quality observations in April–May (c) and December–January (d) on Chongming island during 1995–2018.

2.2.1. Landsat data and preprocessing

The study area is covered by 2 paths/rows (P118R38 and P119R38) of the Landsat Worldwide Reference System (WRS-2) (Fig. 1). We used all the available Landsat 5/7/8 surface reflectance (SR) products between January 1, 1995 and January 1, 2019, which have been archived in Google Earth Engine (GEE), a popular cloud computing platform for planetary-scale remote sensing analysis (Gorelick et al., 2017). The SR datasets have been atmospherically corrected through Landsat Ecosystem Disturbance Adaptive Processing System (LEDAPS) algorithm and Landsat Surface Reflectance Code (LaSRC) algorithm, respectively (Masek et al., 2006; Vermote et al., 2016). The bad-quality observations, including clouds, cirrus, and cloud shadows were identified, according to the pixel quality assessment (pixel_qa) generated from the CFMask algorithm (Zhu and Woodcock, 2012). All the Landsat image pre-processing tasks were carried out on the GEE platform. Fig. 3 shows the annual distributions of all the available Landsat images by sensors (Fig. 3a) and by seasons (Fig. 3b) during 1995–2018. We also counted the numbers of good-quality observations of individual pixels in April–May (Fig. 3c) and in December–January (Fig. 3d) in each year during 1995–2018. The majority of pixels had at least one good observation in April–May (> 93.7% pixels) and in December–January (> 93.9% pixels) during 1995–2018.

The time series Landsat SR data with good-quality observations were used to calculate three vegetation indices (VIs): Normalized Difference Vegetation Index (NDVI) (Tucker, 1979), Enhanced Vegetation Index (EVI) (Huete et al., 2002), and Land Surface Water Index (LSWI) (Xiao et al., 2005). NDVI is closely related to leaf area index (LAI), and EVI is more responsive to chlorophyll content in the canopy. Both NDVI and EVI are widely used in the studies of land surface phenology (Zhang et al., 2003). LSWI is a spectral indicator of canopy and soil moisture, and a change from positive LSWI value to negative LSWI value is used to represent a state of change from green leaf to senescent leaf (Xiao et al., 2009). These three vegetation indices are calculated using following equations:

$$NDVI = \frac{\rho_{NIR} - \rho_{Red}}{\rho_{NIR} + \rho_{Red}} \quad (1)$$

$$EVI = 2.5 \times \frac{\rho_{NIR} - \rho_{Red}}{\rho_{NIR} + 6 \times \rho_{Red} - 7.5 \times \rho_{Blue} + 1} \quad (2)$$

$$LSWI = \frac{\rho_{NIR} - \rho_{SWIR}}{\rho_{NIR} + \rho_{SWIR}} \quad (3)$$

where ρ_{Blue}, ρ_{Red}, ρ_{NIR}, ρ_{SWIR} are the surface reflectance values of blue (450–520 nm), red (630–690 nm), near-infrared (NIR: 760–900 nm), and shortwave-infrared (SWIR: 1550–1750 nm) bands.

2.2.2. In-situ field survey data for training

We collected and organized *in-situ* data from different sources. First, two major field surveys on Chongming island were carried out in mid-July of 2012 and August to September of 2015, taking many GPS field photos. Second, a transect perpendicular to the levee through east to west was established in 2005, and nowadays there are totally five transects in the CDNNR. Those transects provided frequent vegetation information and geo-referenced field photos. According to field photos and very high spatial resolution (VHSR) imagery from Google Earth (GE) around 2012, we selected and digitized the training Region of Interests (ROIs) (Fig. 1). Although some field photos were taken in 2015, they also offered useful references to vegetation types through visual interpretation. We collected training ROIs across the *Spartina* saltmarsh (17 ROIs with a total of 610 pixels) and other saltmarshes dominated by *Phragmites* and *Scirpus* (10 ROIs with a total of 68 pixels).

2.3. Phenology of Spartina and other saltmarshes on Chongming island

We collected time series *in-situ* phenological observations in 2018–2019 for one *Spartina* site from an automated digital camera (Brinno BCC200). The camera has high performance HDR video sensor that generates a real time-lapse video at 5-second interval. We selected one photo with best quality per month to construct the growth cycle of *Spartina*, which serves as reference to interpret the time series Landsat data in tracking saltmarsh vegetation phenology (Fig. S1). According to the ground observation, *Spartina* starts to green-up in late April, grows rapidly from June to early September, and senesces in late December.

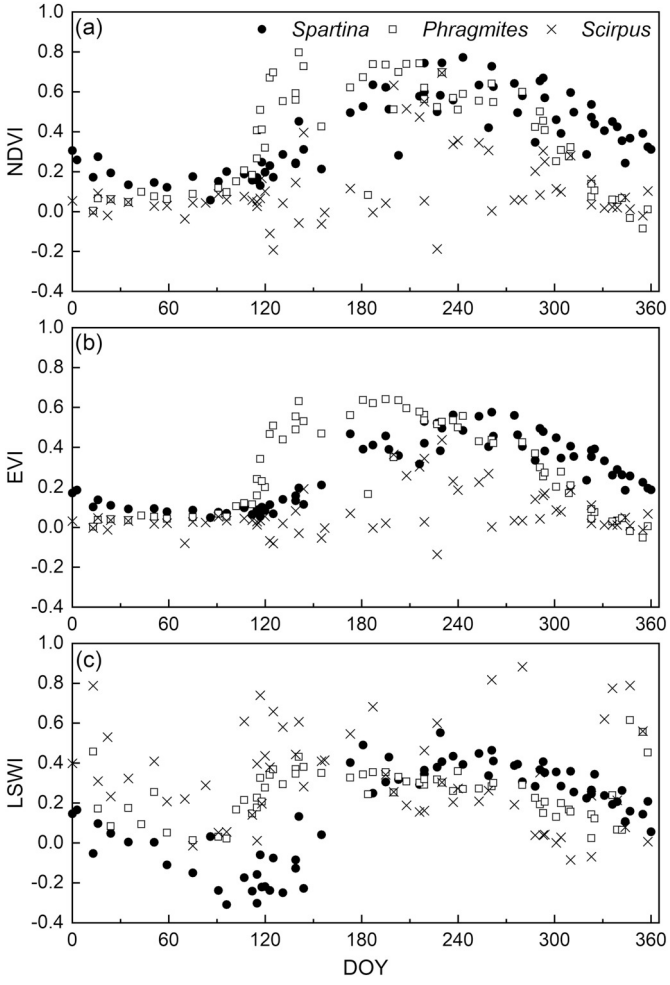

Fig. 4. The seasonal dynamics of Landsat (TM/ETM+/OLI)-derived vegetation indices (a) NDVI, (b) EVI, and (c) LSWI at the three *Spartina*, *Phragmites* and *Scirpus* saltmarsh sites during 2008–2012. The landscapes of these three saltmarsh sites are shown in Fig. 1a.

Time series VIs derived from Landsat 5/7/8 images from 2008 to 2012 were used to depict the seasonal dynamics and interannual variation of three saltmarsh types at the pixel scale. We selected three sites (Fig. 1a), which were dominated by *Spartina*, *Phragmites* and *Scirpus* saltmarshes during 2008–2012, respectively, according to the field photos and VHSR images in GE (Fig. 1b-g). *Phragmites and Scirpus* saltmarshes are the main native saltmarsh communities. The seasonal dynamics of vegetation indices of *Spartina* saltmarsh differed from those of *Phragmites* and *Scirpus* saltmarshes in two periods (Fig. 4): (1) April to May (spring; plant green-up) and (2) December to January (winter; plant senescence). The detailed phenological analysis for these three saltmarshes is given in Section 3.1.

2.4. A pixel- and phenology-based algorithm for identifying and mapping Spartina saltmarsh

The workflow diagram for identifying and mapping spatial-

temporal dynamics of *Spartina* saltmarsh on Chongming island during 1995–2018 is given in Fig. 2. For each year, we first delineated the intertidal zone, which stretches between the low-tide waterline, mudflats, wetland, and high-tide waterline. Second, we identified and mapped the coastal vegetation area. Third, we identified *Spartina* saltmarsh from other saltmarshes among the coastal vegetation maps. Since the ecological project was started in 2013, we used 2012 as the baseline year to first produce the intertidal zone, coastal vegetation area, and *Spartina* saltmarsh maps. We generated annual maps of *Spartina* saltmarsh during 1995–2018, and used them to analyze the expansion process (1995–2012) and removal dynamics (2013–2018) of *Spartina* saltmarsh on Chongming island. The detailed procedure is described below.

2.4.1. Delineating intertidal zone

Spartina encroachment into native saltmarshes is the main focus in this study, thus we are more concerned with the vegetation distributed in the intertidal zone. We delineated the coastline by visual interpretation and manual digitization of very high spatial resolution images, and then excluded the inland area by specifying intertidal buffer zone. A 6-km outward coastline buffer zone was generated to delineate the intertidal range. The boundary of buffer zone was modified in some regions where the border intersects with Jiangsu province and two southern islands (Hengsha island and Changxing island). Delineation of intertidal zone as potential distribution regions was the first step to assist for *Spartina* saltmarsh extraction.

2.4.2. Identifying coastal vegetation area

Effective discrimination of *Spartina* saltmarsh starts with the accurate coastal vegetation maps. In an earlier study, we had developed a decision tree classification algorithm for mapping coastal vegetation in China, based on Landsat TM/ETM+/OLI imagery (Wang et al., 2018; Wang et al., 2020). As a follow-up work, we produced coastal vegetation maps of Chongming island using the same algorithm. Individual good-quality observations in a year were first identified as green vegetation or not, using Eq. (4), and then vegetation frequency in a year is calculated, using Eq. (5).

$$Vegetation = NDVI \geq 0.2 \cap EVI \geq 0.1 \cap LSWI > 0 \quad (4)$$

$$VF = \frac{N_{Vegetation}}{N_{Good}} \quad (5)$$

where VF is green vegetation frequency scaled to 0 and 1 for a pixel in a year, $N_{Vegetation}$ is the number of observations identified as green vegetation in a year, N_{Good} is the number of good-quality observations in a year. The frequency threshold value of 0.05 was used to classify a pixel as coastal vegetation area (VF $\geq$ 0.05) or non-vegetated area such as tidal flats (VF $<$ 0.05) (Wang et al., 2018; Wang et al., 2020). The resultant annual coastal vegetation maps on Chongming island were used as the baseline map for the phenology-based identification and mapping of *Spartina* saltmarsh in the next step.

2.4.3. Identifying Spartina saltmarsh

As an invasive plant with high competitiveness, *Spartina* could rapidly dominate and replace the native saltmarsh communities, forming large patches on the ground. A pixel- and phenology-based algorithm was developed for *Spartina* saltmarsh mapping based on 30-m Landsat data. The two key phenology features of *Spartina* saltmarsh (Fig. 4) were used in the phenology-based algorithm: (1) later green-up in spring and (2) later senescence in winter. In April–May, *Spartina* saltmarsh had low NDVI, EVI and LSWI values, while the other saltmarshes (*Phragmites* and *Scirpus*) started to green-up with higher VIs values especially in LSWI ($>$ 0). We calculated the mean value of LSWI during April to May ($LSWI_{mean(Apr\text{-}May)}$) for individual pixels, and the histogram suggested that $LSWI_{mean(Apr\text{-}May)}$ less than 0 could discriminate *Spartina* from the other saltmarshes (see Section 3.1 for more details). In December–January, NDVI and EVI showed large differences between *Spartina* and the other two saltmarshes. The relatively high NDVI ($>$ 0.2), EVI ($>$ 0.1) and LSWI ($>$ 0) values at the *Spartina* pixels represented green vegetation signal, which was another critical indicator to identify *Spartina* saltmarsh. The green vegetation here is consistent with the concept presented in Section 2.4.2. We counted the number of observations that were identified as green vegetation in December–January and calculated the green vegetation frequency ($VF_{Dec\text{-}Jan}$). Approximately 99% of *Spartina* saltmarsh pixels had $VF_{Dec\text{-}Jan} > 0$ (see Section 3.1 for more details). Therefore, the decision rules for identifying *Spartina* saltmarsh from the coastal vegetation map were $LSWI_{mean(Apr\text{-}May)} \leq 0$ and $VF_{(Dec\text{-}Jan)} > 0$, as shown in Eq. (6).

$$Spartina\ saltmarsh = LSWI_{mean(Apr-May)} \leq 0 \cap VF_{(Dec-Jan)} > 0 \quad (6)$$

where $LSWI_{mean(Apr\text{-}May)}$ is the mean value of LSWI in April–May, and $VF_{(Dec\text{-}Jan)}$ is the green vegetation frequency in December–January, calculated as the ratio of the number of observations identified as green vegetation to the number of good quality observations in December–January, similar to Eq. (5).

2.5. Accuracy assessment of the Spartina saltmarsh maps

For the validation datasets we first used the stratified random sample function in GEE to define and collect samples. When the sample size in each category is in proportion to the surface area of that category, the accuracy assessment is reliable (Olofsson et al., 2014; Olofsson et al., 2013). As *Spartina* saltmarsh and the other saltmarshes (Non-*Spartina*) had comparatively similar-sized areas, we set the same number of random points (100 points) for both categories. Next, the validation ROIs were delineated with a 30-m circle buffer of the random sampling points in ArcGIS, exported as Keyhole Markup Language (KML) file, and loaded into Google Earth. The VHSR imagery in GE is an effective data source to validate the land classification results (Huang et al., 2010; Kennedy et al., 2010). We inspected each ROI through visual interpretation of VHSR images and the geo-referenced photos. The ROIs without clear land cover information due to unavailable reference or cloud interference were excluded. In the VHSR images, the *Spartina* patches could be clearly identified from their clumpy configuration (Fig. 1b). Owing to the high invasion rate, the spatial distribution of *Spartina* saltmarsh was subject to interannual variation, making it necessary to take an annually intensive accuracy assessment. However, because of the limited numbers of VHSR images and field photos, we only assessed the accuracies of mapping results in four years (i.e., 2012–2014, and 2016). The total number of validation samples for *Spartina* and Non-*Spartina* were 71 and 61 in 2012, 75 and 80 in 2013, 82 and 86 in 2014, 61 and 91 in 2016, respectively (Fig. S2). The confusion matrix of *Spartina* saltmarsh maps was calculated to estimate the accuracy of the maps. Following the previous study (Olofsson et al., 2013), we adjusted accuracies of the resultant maps by considering the area of each category, and the area estimates were also corrected based on the area-adjusted accuracies.

2.6. Comparison with other available Spartina saltmarsh datasets

Besides the validation by *in-situ* data and VHSR images, a comparison between our Landsat- and phenology-based *Spartina* saltmarsh maps and other *Spartina* saltmarsh datasets would be informative. Unfortunately, no other *Spartina* saltmarsh maps are available to the public for spatial comparison. A couple of publications reported only the area estimates of *Spartina* saltmarsh, thus we did the areal comparison in this study. The Resource Monitoring Reports from Shanghai Chongming Dongtan National Nature Reserve were published annually during 2006–2015, and provided data of plants, macrobenthos, zooplankton, fishes, and waterfowl (http://www.dongtan.cn/). In most cases, they analyzed either satellite images (e.g., HJ-1a/b and ZY-02C/3) or airborne images with maximum likelihood supervised

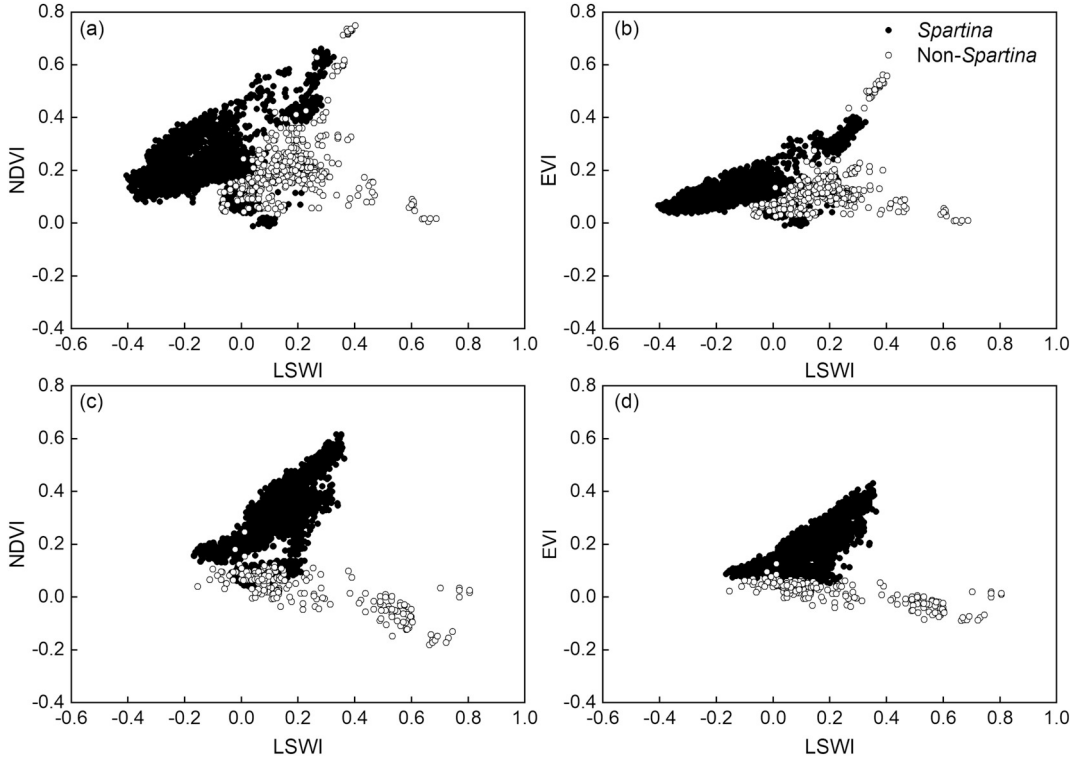

Fig. 5. The two-dimensional scatterplots between greenness-related indices (NDVI, EVI) and water-related index (LSWI) of *Spartina* and Non-*Spartina* saltmarshes based on the training dataset in April–May (spring season) (a, b) and December–January (winter season) (c, d) during 2010–2012.

classification method for monitoring and reporting the dominant plant communities. The classification results were corrected with field survey data and validated by various sources (e.g., aerial photos) with an accuracy over 85%.

3. Results

3.1. Phenology of Spartina saltmarsh as observed by Landsat time series images

We combined all the available good-quality observations during 2008–2012 at three sites (Fig. 1a) to show the seasonal dynamics of NDVI, EVI and LSWI of *Spartina*, *Phragmites* and *Scirpus* saltmarshes (Fig. 4). In winter, NDVI and EVI values at these three sites were very low and in similar range during February–March. In spring, NDVI, EVI and LSWI values at the *Phragmites* site rose substantially during late April-early May, which were driven by new leaf flush and rapid growth of leaves. LSWI values at the *Scirpus* site also rose substantially in late April-early May. In comparison, NDVI, EVI and LSWI values at the *Spartina* site remained to be very low in late April-early May, including LSWI remained negative value (< 0). The seasonal dynamics of NDVI, EVI and LSWI in spring season suggested that *Phragmites* and *Scirpus* started to green-up in late April and early May, and *Spartina* started to green-up in late May. The *Phragmites* and *Scirpus* saltmarsh sites reached their highest NDVI, EVI and LSWI values in the early summer, but NDVI, EVI and LSWI values at the *Spartina* saltmarsh site peaked at the late summer. NDVI and EVI values at the *Phragmites* and *Scirpus* sites dropped substantially by November–December, reaching NDVI < 0.2 and EVI < 0.1, which were driven by leaf senescence. In comparison, the *Spartina* site still remained green in November–December, having relative higher NDVI (> 0.2) and EVI (> 0.1) values. The seasonal dynamics of NDVI, EVI, and LSWI in fall and winter seasons suggested that *Pragmites* and *Scipus* started to experience leaf senescence in November and December, and *Spartina* did not enter senescence until January of the next year. These phenological characteristics as observed by three vegetation indices suggested that April–May and December–January are two temporal periods that we can use Landsat images to separate *Spartina* saltmarsh from *Phragmites* and *Scirpus* saltmarshes on Chongming island.

Fig. 5 shows the relationships between greenness-related indices (NDVI, EVI) and water-related index (LSWI) in spring (April–May) and winter (December–January) during 2010–2012 based on the training dataset (see 2.2.2 section). In spring, most observations of the *Spartina* saltmarsh pixels had negative LSWI values, while most observations of the other saltmarshes (*Pragmites* and *Scirpus*) pixels had positive LSWI values (Fig. 5a-b). In winter, most observations of the *Spartina* saltmarsh pixels had NDVI values greater than 0.2, EVI values greater than 0.1, and LSWI values greater than 0, while most observations of the other saltmarshes pixels had NDVI values smaller then 0.2 and EVI values smaller than 0.1 (Fig. 5c-d). These scatterplots also illustrated the potential to separate *Spartina* saltmarsh from the other two native saltmarshes by vegetation indices in the spring and winter seasons.

We also used the training data and the histograms to explore and visualize the separability between *Spartina* and the other two saltmarshes in spring (April–May) and winter (December–January) during 2010–2012 (Fig. 6). In April–May, LSWI was a more effective indicator than NDVI and EVI for identifying *Spartina* saltmarsh (Fig. 6a-c). The mean value of LSWI in April–May ($LSWI_{mean(Apr\text{-}May)}$) indicated that a threshold of 0 could be used for identifying *Spartina* saltmarsh (Fig. 6d). In December–January, NDVI and EVI were more effective indicators than LSWI for identifying *Spartina* saltmarsh (Fig. 6e-g). The histogram of green vegetation frequency in December–January ($VF_{(Dec\text{-}Jan)}$) showed that the threshold of 0 can separate 99.7% of *Spartina* saltmarsh pixels ($VF_{(Dec\text{-}Jan)} > 0$) from 98.5% of Non-*Spartina* saltmarsh pixels ($VF_{(Dec\text{-}Jan)} < 0$) (Fig. 6h). The results from the training datasets clearly illustrated phenological differences between *Spartina* saltmarsh and the

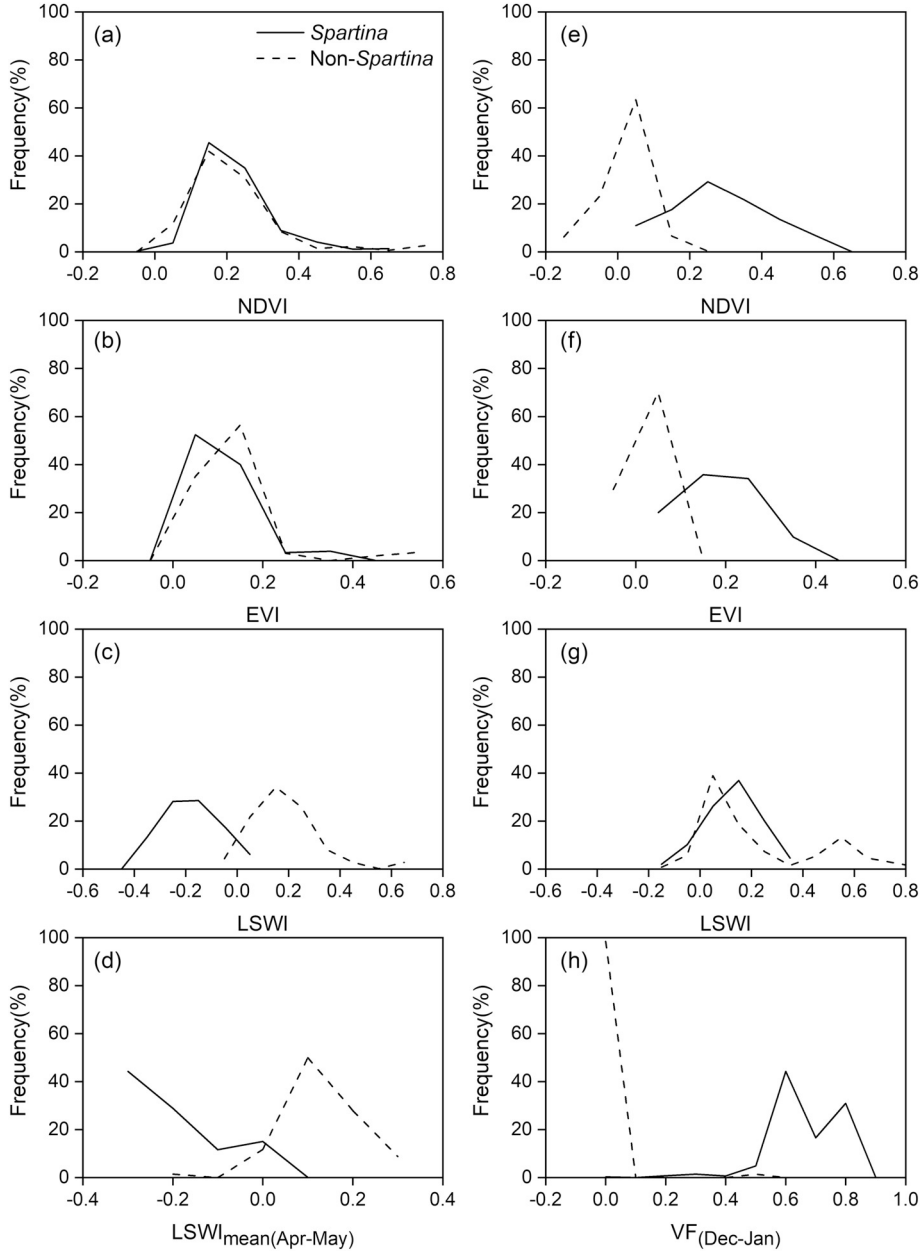

Fig. 6. The histograms of vegetation indices (NDVI, EVI, and LSWI), $LSWI_{mean(Apr\text{-}May)}$ and $VF_{(Dec\text{-}Jan)}$ of *Spartina* and Non-*Spartina* saltmarshes based on the training dataset in April–May (a-d) and December–January (e-h) during 2010–2012.

other saltmarshes (*Phragmites* and *Scirpus*), which were the foundation for our pixel- and phenology-based algorithm to identify and map *Spartina* saltmarsh on Chongming island.

3.2. Annual map of coastal vegetation and Spartina saltmarsh on Chongming island in 2012

According to the annual map of coastal vegetation and *Spartina* saltmarsh in 2012 (Fig. 7), there were 2067, 1312 ha, and 1253 ha *Spartina* saltmarsh in 2012 on Chongming island, CDNNR, and DEPA, respectively. *Spartina* encroachment mainly occurred in the northern and northeastern part of Chongming island, which can be seen as two encroachment clusters (see box 1 and 2 in Fig. 7a). The northern cluster was located where tidal flats had been expanding outward over years, and *Spartina* saltmarsh gradually colonized newly emerging tidal flats. The northeastern cluster was spatially in line with the artificial *Spartina* planting history, accounting for ~56% of the total *Spartina* saltmarsh area on Chongming island.

3.3. Accuracy assessment of the Spartina saltmarsh maps

We carried out the accuracy assessment for annual maps of *Spartina* saltmarsh in 2012, 2013, 2014, and 2016, based on the availability of the validation datasets (Table 2). The overall accuracies (OA) were 0.93, 0.94, 0.91, and 0.94, and the Kappa coefficients were 0.86, 0.87, 0.82, and 0.88 in 2012, 2013, 2014, and 2016, respectively. The *Spartina* saltmarsh had producer accuracies (PA) of 0.90, 0.91, 0.89, and 0.92, and user accuracies (UA) of 0.99, 0.96, 0.93, and 0.93 in these four maps. We also calculated the error-adjusted producer's (APA), user's (AUA) and overall (AOA) accuracies (Olofsson et al., 2013). The adjusted OAs (AOA) ranged between 0.90 and 0.94, which were slightly lower than the unadjusted OAs (0.91–0.94). The adjusted

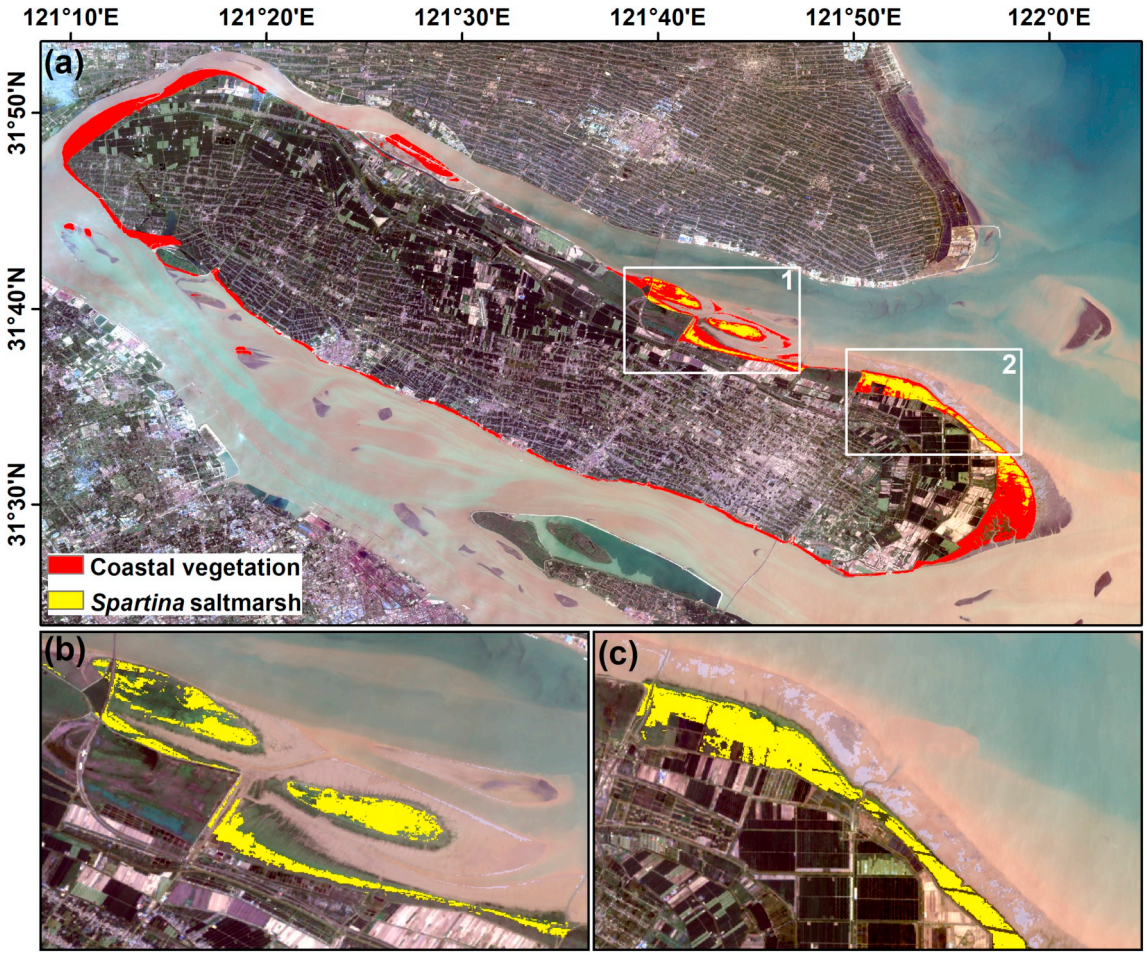

Fig. 7. The coastal vegetation and *Spartina* saltmarsh maps in 2012 on Chongming island, China. (a) annual map in 2012, (b, c) zoom-in view of two regions labeled as 1, 2 in (a), respectively.

PAs (APA) dropped substantially to 0.70, 0.66, 0.59, and 0.46, respectively. This discrepancy between PA and APA could be explained by the variation in estimation weights associated with the areas of each category. We calculated the *Spartina* saltmarsh mapping areas (Area) and also error-adjusted estimated areas (EArea) with 95% confidence interval from these four annual maps. The adjusted areas for *Spartina* saltmarsh increased substantially, for example, increasing from 2119 ha to 3082 ha in 2013 on Chongming island.

3.4. Expansion and removal dynamics of Spartina saltmarsh during 1995–2018

To reduce uncertainties caused by image quality or other factors in individual years, we aggregated annual maps of *Spartina* saltmarsh within multi-year (three to five years) interval and then reported its maximum extent at multi-year epochs (1995–1999, 2000–2004, 2005–2009, 2010–2012) during 1995–2012, which is considered as *Spartina* expansion period before the *Spartina* removal project was started in December 2013. Fig. 8a shows the *Spartina* saltmarsh expansion dynamics at 30-m spatial resolution in four multi-year epochs. The spatial-temporal analysis showed that Chongming island experienced a significant *Spartina* encroachment and expansion in the north and northeast part. The expansion process of *Spartina* saltmarsh in the north and northeast of Chongming island was depicted in spatial detail (Fig. 8b-c). *Spartina* saltmarsh had clearly extended into the sea side over the past two decades, which was in accordance with the trajectory of tidal flats (Wang et al., 2018). It also showed the opposite direction of expansion toward high mudflat in some regions, replacing the native

Table 2
A summary for the accuracy assessment for annual maps of *Spartina* saltmarsh and the other saltmarshes in 2012, 2013, 2014, and 2016 on Chongming island. Producer's (PA), user's (UA) and overall (OA) accuracies and error-adjusted producer's (APA), user's (AUA) and overall (AOA) accuracies. This table also shows the mapped areas (Area) and estimated areas (EArea) with 95% confidence interval.

Year	Class	PA	UA	OA	Area(ha)	APA	AUA	AOA	EArea(ha)
2012	*Spartina*	0.90	0.99	0.93	2067.26	0.70	0.99	0.90	3173.57 ± 756.83
	Non-*Spartina*	0.98	0.87			1.00	0.87		
2013	*Spartina*	0.91	0.96	0.94	2119.09	0.66	0.96	0.92	3082.16 ± 767.51
	Non-*Spartina*	0.96	0.91			0.99	0.91		
2014	*Spartina*	0.89	0.93	0.91	1809.79	0.59	0.93	0.90	2856.55 ± 755.51
	Non-*Spartina*	0.93	0.90			0.99	0.90		
2016	*Spartina*	0.92	0.93	0.94	728.78	0.46	0.93	0.94	1469.86 ± 691.30
	Non-*Spartina*	0.96	0.95			1	0.95		

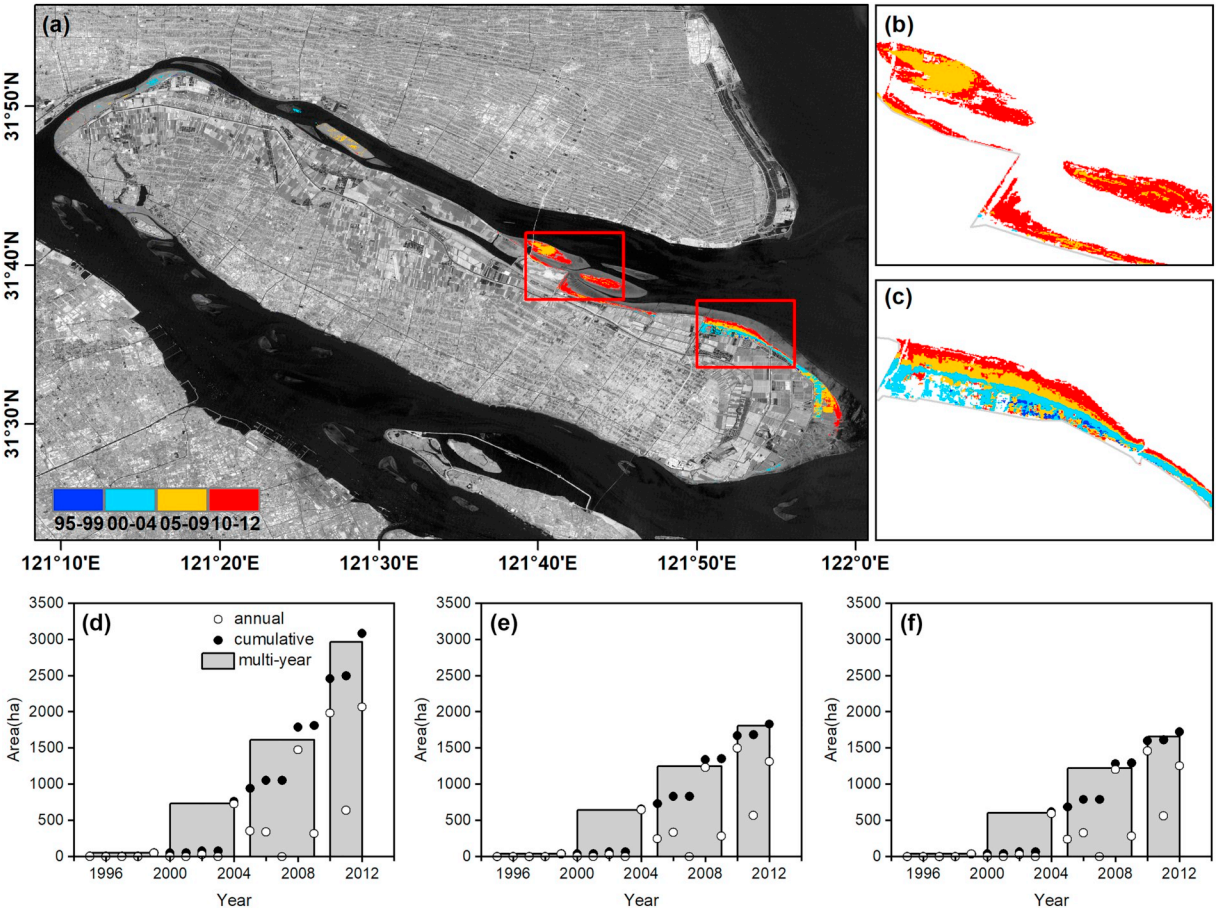

Fig. 8. The expansion dynamics of *Spartina* saltmarsh during 1995–2012 on Chongming island. (a) spatial distribution of *Spartina* saltmarsh at multi-year epochs, (b, c) zoom-in view for the region highlighted by the red box in (a). The annual, multi-year, and cumulative areas of *Spartina* saltmarsh in the Chongming island (d), CDNNR (e), and DEPA (f) during 1995–2012. (For interpretation of the references to colour in this figure legend, the reader is referred to the web version of this article.)

saltmarshes such as *Phragmites* saltmarsh. We calculated the annual, multi-year, and cumulative areas of *Spartina* saltmarsh during 1995–2012 in the Chongming island (Fig. 8d), CDNNR (Fig. 8e), and DEPA (Fig. 8f), respectively. The *Spartina* encroachment includes three stages: colonization, rapid expansion, and successful invasion. In the 1990s and early 2000s, *Spartina* was intentionally planted and naturally propagated with very small patches that hardly detected from the Landsat images. *Spartina* encroachment had entered successful invasion phase since the mid-2000s and then expanded linearly and continuously from ~729 ha in 2004 to ~2067 ha in 2012 on Chongming island (Fig. 8d).

The ecological engineering project of controlling *Spartina* was implemented in 2013–2016. Based on the experimental results for removing *Spartina* plants in 2012 at the experimental fields, staff at the CDNNR used a procedure that first cut *Spartina* plants at the flowering stage and then inundate (flood) the fields over 6 months, which would ensure full death of *Spartina* plants. The annual *Spartina* saltmarsh maps during 2013–2018 showed the spatial-temporal changes of *Spartina* saltmarsh (Fig. 9a-f). *Spartina* saltmarsh area decreased substantially in the project area (DEPA) during 2013–2016 at the rate of ~440 ha per year ($P < 0.01$) (Fig. 9i), which is in line with the project's cutting plan. According to the reports from the engineering project, *Spartina* saltmarsh area was reduced by more than 95% in 2016. The Landsat-based *Spartina* saltmarsh maps also showed that the *Spartina* saltmarsh area was reduced by ~99% during 2013–2016. The agreement between the project's report and our Landsat-based analysis demonstrates the potential and capacity of *Spartina* saltmarsh monitoring by using Landsat images and the algorithm.

4. Discussion

4.1. Area estimates and spatial-temporal dynamics of Spartina saltmarsh

According to our Landsat-based annual maps of *Spartina* saltmarsh on Chongming island during 1995–2012, *Spartina* saltmarsh area had a slowly increasing phase in the 1990s and a rapidly increasing phase in the 2000s (Fig. 8d-f). In our literature review, we found only two studies that reported *Spartina* saltmarsh area on Chongming island, 1239 ha in 2003 (Li et al., 2006) and 3132 ha in 2007 (Lu and Zhang, 2013), which were much larger than our estimates. A few studies reported *Spartina* saltmarsh area in the CDNNR (Huang, 2009; Lin et al., 2018; Luo, 2019; Wang, 2007), and the area estimates of *Spartina* saltmarsh varied among these publications. According to the study by Wang (2007), *Spartina* saltmarsh area in the CDNNR was 466 ha in 2000, 579 ha in 2002, 1112 ha in 2003 and 1441 ha in 2004. Another study by Huang (2009) showed that *Spartina* saltmarsh area in the CDNNR was 187 ha in 2000, 932 ha in 2003, 1377 ha in 2008 *Spartina* saltmarsh. *Spartina* saltmarsh area estimates from Lin et al. (2018) was 345 ha in 2000, 1114 ha in 2003, 1184 ha in 2007, 463 ha in 2009 and 837 ha in 2013. In a study of mapping *Spartina* saltmarsh along the coastal zones of mainland China, Liu et al. (2018) analyzed 43 Landsat 8 OLI images from 2014 to 2016 and reported 965 ha of *Spartina* saltmarsh in the CDNNR in 2015, which is higher than our mapping result (668 ha) using images from 2015. Ge et al. (2013) developed a process-based grid model to simulate *Spartina* expansion in the CDNNR and reported that *Spartina* saltmarsh area increased from 107 ha in 2001 to 922 ha in 2006 and then slowed down in 2007–2008. Our

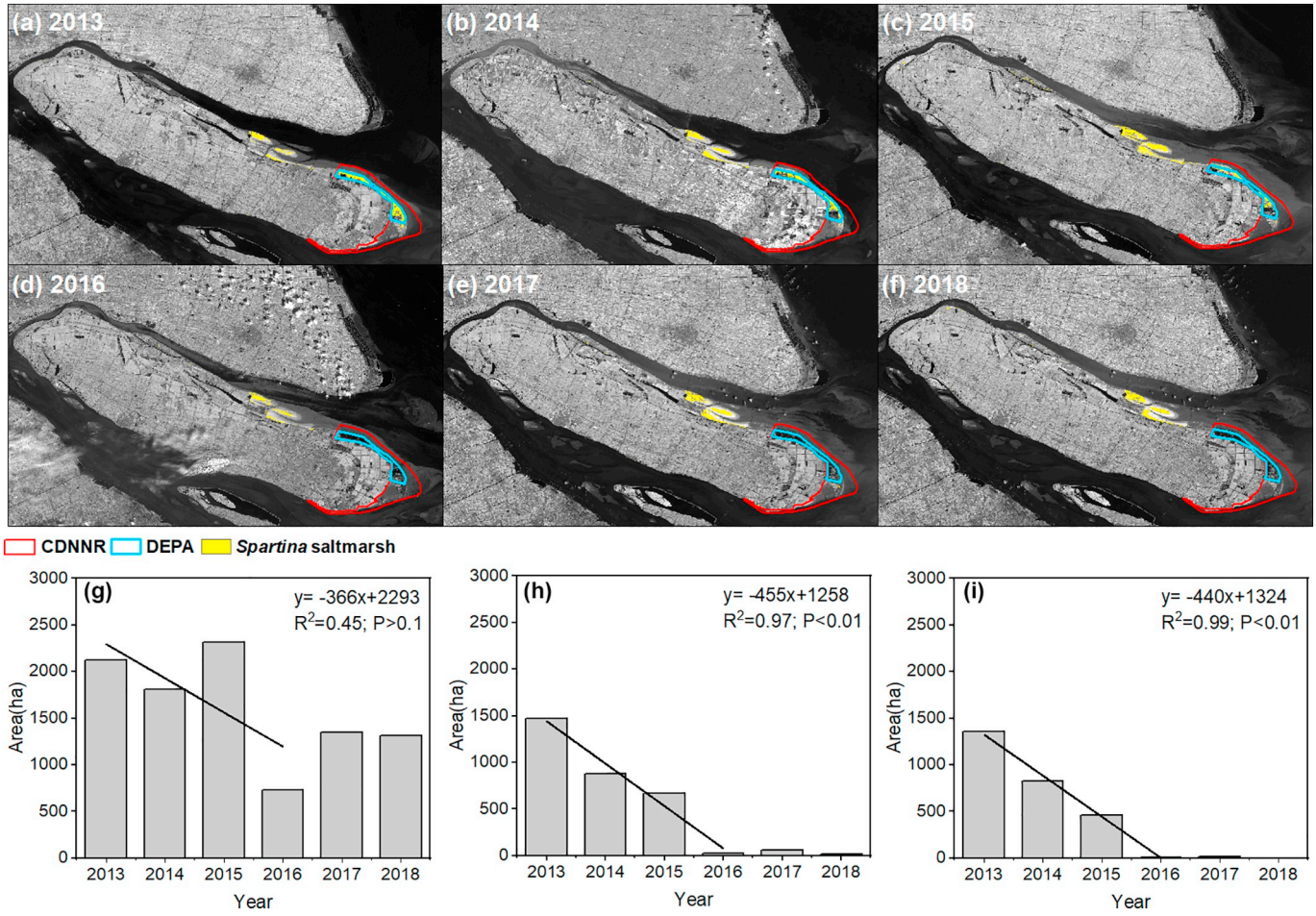

Fig. 9. The removal dynamics of *Spartina* saltmarsh during 2013–2018 on Chongming island. (a-f) annual maps of *Spartina* saltmarsh, (g-i) annual area of *Spartina* saltmarsh in the Chongming island, CDNNR and DEPA, respectively. The red and blue polygons represent the CDNNR and DEPA boundary. The linear regression model was applied for the *Spartina* saltmarsh area data in 2013–2016. (For interpretation of the references to colour in this figure legend, the reader is referred to the web version of this article.)

results (Fig. 8e) show that the *Spartina* saltmarsh area continued to increase linearly up to 2012. The dramatic increase of *Spartina* saltmarsh in the 2000s was the result of competitive replacement of native *Phragmites* by invasive *Spartina*, driven by high salinity (Li et al., 2009). The CDNNR department reported that in 2012 the reserve had a total area of 4265 ha saltmarshes, including 1958 ha *Spartina* saltmarsh (accounting for ~45.9% of the total saltmarsh area), which are approximately 30% larger than the area estimates from our Landsat-based annual map in 2012 (1312 ha). However, when we overlaid all annual maps of *Spartina* saltmarsh in 2011–2013, the resultant maximum area of *Spartina* saltmarsh is 1650 ha. It should be pointed out that the CDNNR monitoring report classified saltmarsh vegetation by visual interpretation of very high spatial resolution images (e.g., ZY1-02c), it included small patches of *Spartina* saltmarsh, which are likely to be missed by the pixel-based algorithms and Landsat images.

During those years the ecological engineering project was implemented (2013–2016), our annual maps show that *Spartina* saltmarsh area in Dongtan ecological project area (DEPA) dropped linearly and was 19 ha in 2016 (Fig. 9g). Note that the CDNNR did not report *Spartina* saltmarsh area during 2016–2018. To date, our Landsat-based annual maps during 1995–2018 is the only dataset that documented annual dynamics of *Spartina* saltmarsh in the reserve. Our maps also show that *Spartina* saltmarsh area outside the CDNNR had large increase in 2015 but large drop in 2016 in the 2015/2016 El Nino year (Fig. 9). The large drop of *Spartina* saltmarsh in 2016 was attributed to the die-back and removal by the CDNNR staff (Ma Qiang, personal communication from the CDNNR). By comparing the *Spartina* saltmarsh maps in 2013, 2016, and 2018 (Fig. 9 and S3), we also found a small number of newly emerging *Spartina* saltmarsh patches in 2018. These newly emerging *Spartina* invasions in the DEPA and the large *Spartina* saltmarsh area outside the CDNNR clearly suggest that the CDNNR and researchers need to pay close attention to the remaining *Spartina* populations and develop a continuous monitoring and management plan for the CDNNR.

4.2. The potential of the pixel- and phenology-based algorithm for Spartina saltmarsh mapping

Many studies have used single or multi-date satellite images to identify and map *Spartina* saltmarsh in China (Table 1). Most of these studies calculated the spatial statistics of spectral bands and vegetation indices and used supervised or unsupervised classification algorithms to classify *Spartina* saltmarsh and generate maps of *Spartina* saltmarsh (Huang and Zhang, 2007a; Liu et al., 2016; Zhang et al., 2017). The metrics and parameters in these algorithms are affected by selected images used in the calculation of the spatial statistics of individual images, as saltmarsh plants have strong and diverse phenology in a year. Numerous studies have shown that vegetation phenology can be well depicted by time series vegetation indices from the MODIS sensors that acquire images at daily interval (Wu et al., 2017; Zhang et al., 2006; Zhang et al., 2003). In this study, our results show that there are reasonable numbers of time series Landsat images, which were acquired

at 16-day interval, to describe phenology of saltmarshes on Chongming island, China (Fig. 4). This can also refine the studies that use single or multi-date images, as researchers could now carry out phenological analysis of all Landsat images in a year and then select appropriate images for data analysis.

Our study investigated phenology of *Spartina* saltmarsh and other saltmarshes (*Phragmites* and *Scirpus*) on Chongming island, and the unique phenological characteristics of these saltmarshes in spring green-up and winter senescence stages were identified (Fig. 5). This is similar to a previous study (Ai et al., 2017) that tracked the phenological variations of *Spartina* and native species by using GF-1 WFV imagery. We also found that both greenness-related vegetation indices (NDVI, EVI) and water-related vegetation indices (LSWI) are useful to separate invasive *Spartina* saltmarsh from native *Phragmites* and *Scirpus* saltmarshes on Chongming island, which is consistent with our previous studies that aimed to identify and map inland natural and agricultural wetlands (Dong et al., 2015; Dong et al., 2016; Xiao et al., 2006; Xiao et al., 2005). Both NDVI and LSWI were also used in recent studies that identified and mapped *Spartina* saltmarsh in China (Liu et al., 2018).

As described in Table 1, we developed a mapping tool that uses time series Landsat images and a pixel- and phenology-based algorithm to identify and map *Spartina* saltmarsh over years. The simple algorithms are built upon the phenological differences between *Spartina* saltmarsh and other saltmarshes (*Phragmites* and *Scirpus*) in spring (April–May) and winter (December–January) (Fig. 5). Several studies that used single or multi-date Landsat images also considered phenological stages and tidal level and selected images in spring and winter (Liu et al., 2018; Mao et al., 2019; Wang et al., 2015). In our study, we used all the available time series Landsat images, in this way, we have more good-quality observations and could better capture phenological differences between *Spartina* and other saltmarshes in a year. The pixel- and phenology-based mapping algorithm and time series Landsat data have been used to identify water-related land cover types, including open surface water (Zou et al., 2017; Zou et al., 2018), paddy rice (Dong et al., 2015; Dong et al., 2016; Zhang et al., 2015) and coastal wetlands (Wang et al., 2018; Wang et al., 2020). The spatial-temporal dynamics of *Spartina* saltmarsh on Chongming island reported from this study showcases that the human management of invasive species (e.g., ecological engineering project) could be accurately assessed by the time series Landsat images and pixel- and phenology-based mapping algorithm.

4.3. Sources of errors and limitations of the resultant annual maps of *Spartina* saltmarsh

In general, the quality and accuracy of land cover map is affected by a number of factors: (1) good-quality image data, (2) availability and quality of *in-situ* training sample data, (3) algorithms, and (4) definition of land cover type (Foody, 2002; Gong et al., 2012). The annual maps of *Spartina* saltmarsh from this study also have a number of sources of errors and limitations. First, the implementation of pixel- and phenology-based algorithm in coastal wetlands was largely restricted by the amount of good-quality observations in specified phenological phases, which depends upon observation frequency (16-days revisit cycle) and data quality (e.g., cloud and cloud shadow). For example, more than 80% of the pixels had zero good-quality observation in April–May of 2003 and December–January of 2007 (Fig. 3), which would result in high omission errors in the annual maps of 2003 and 2007. For this reason, we also reported multi-year area estimates (e.g., 1995–1999, 2000–2004, 2005–2009, 2010–2012) and combined annual *Spartina* saltmarsh maps to generate cumulative *Spartina* saltmarsh extent for documenting expansion dynamics of *Spartina* saltmarsh (Fig. 8). Second, there are some small patches of *Spartina* saltmarsh, thus mixed-pixel phenomenon is unavoidable in Landsat 30-m spatial resolution imagery. A pixel may be a pure pixel or a mixed pixel with plants, soil, and sea water. The process of *Spartina* plants encroaching into a new pixel involve generally four phases: introduction, establishment, expansion, and dominance (Vaz et al., 2018). During the stage of introduction and establishment, *Spartina* often has small canopy and occupies small fraction area within 30-m pixels. It is a challenge to classify pixels with mixed vegetation species in the field of land-cover mapping (Gong et al., 2012; Herold et al., 2008; Wang et al., 2017). In our pixel- and phenology-based study, we aimed to identify those pixels dominated by *Spartina*, which means that the *Spartina* will only be detectable once it reaches high coverage (relative to pixel size) to influence the phenological signal. That could be one reason that our *Spartina* saltmarsh estimate area is lower than the area estimates from the annual reports of the Chongming Dongtan National Nature Reserve. Sentinel-2A/2B data together constitute time series data at higher temporal frequency (5-day) and spatial resolution (10-m, 20-m), thus, future effort in mapping and monitoring *Spartina* saltmarsh should combine both Landsat and Sentinel-2 images together. Third, LSWI, calculated as a normalized ratio between NIR and SWIR bands, is useful for measuring both leaf water contents and soil moisture (Chandrasekar et al., 2010). Sea water or moist soils in coastal wetland, such as the spatial-temporal variability of flooding, ponding and soil wetness could also affect NIR and SWIR bands, which might introduce some uncertainties (i.e., omission error) in identifying *Spartina* saltmarsh when using only LSWI-based criterion, especially for those saltmarshes close to seashore. In this study, we used all the available Landsat images, which help reduce the classification errors in the resultant annual and multi-year *Spartina* saltmarsh maps (Table 2).

5. Conclusions

In this study, we used a pixel- and phenology-based algorithm and time series Landsat 5/7/8 images to identify and map *Spartina* saltmarsh. Our case study on Chongming island shows that annual maps of *Spartina* saltmarsh track well the expansion dynamics of *Spartina* saltmarsh during 1995–2012 and removal dynamics during 2013–2016. The resultant annual and multi-year maps of *Spartina* saltmarsh can be used to support various studies that aim to understand the driving factors of *Spartina* saltmarsh dynamics and assess the impacts of *Spartina* saltmarsh expansion on biodiversity, carbon cycle and ecosystem services. The limited number of Landsat images in a year due to the 16-day revisit cycle, tidal dynamics, and mixed coastal vegetation communities could still cause some uncertainties in *Spartina* saltmarsh maps. As time series images from other optical sensors with higher temporal and spatial resolution, for example, Sentinel-2 A/B (10-day revisit cycle, 10-m spatial resolution), become freely available, the proposed algorithm in this study could be by combining both Landsat and Sentinel-2 time series images to identify and map saltmarshes over years in the coastal zones, where billions of people depend upon its goods and services.

Declaration of Competing Interest

The authors declare that they have no known competing financial interests or personal relationships that could have appeared to influence the work reported in this paper.

Acknowledgements

The study was supported by the National Natural Science Foundation of China (41630528 and 41371258), Scientific Research Program of Shanghai Science and Technology Commission (18511102503), U.S. National Institutes of Health (1R01AI101028-02A1), and U.S. National Science Foundation (1911955). We thank Qiang Ma for providing the related information of *Spartina* ecological engineering project in Dongtan National Nature Reserve. We thank all the reviewers for their comments in the earlier versions of the manuscript.

Appendix A. Supplementary data

Supplementary data to this article can be found online at https://doi.org/10.1016/j.rse.2020.111916.

References

Ai, J., Gao, W., Gao, Z., Shi, R., Zhang, C., 2017. Phenology-based Spartina alterniflora mapping in coastal wetland of the Yangtze estuary using time series of GaoFen satellite no. 1 wide field of view imagery. J. Appl. Remote. Sens. 11.

Bradley, B., 2014. Remote detection of invasive plants: a review of spectral, textural and phenological approaches. Biol. Invasions 16, 1411–1425.

Chandrasekar, K., Sesha Sai, M.V.R., Roy, P.S., Dwevedi, R.S., 2010. Land surface water index (LSWI) response to rainfall and NDVI using the MODIS vegetation index product. Int. J. Remote Sens. 31, 3987–4005.

Chung, C.H., 2006. Forty years of ecological engineering with Spartina plantations in China. Ecol. Eng. 27, 49–57.

Chust, G., Galparsoro, I., Borja, A., Franco, J., Uriarte, A., 2008. Coastal and estuarine habitat mapping, using LIDAR height and intensity and multi-spectral imagery. Estuar. Coast. Shelf Sci. 78, 633–643.

Dong, J., Xiao, X., Kou, W., Qin, Y., Zhang, G., Li, L., Jin, C., Zhou, Y., Wang, J., Biradar, C., Liu, J., Moore, B., 2015. Tracking the dynamics of paddy rice planting area in 1986-2010 through time series Landsat images and phenology-based algorithms. Remote Sens. Environ. 160, 99–113.

Dong, J., Xiao, X., Menarguez, M.A., Zhang, G., Qin, Y., Thau, D., Biradar, C., Moore, B., 2016. Mapping paddy rice planting area in northeastern Asia with Landsat 8 images, phenology-based algorithm and Google earth engine. Remote Sens. Environ. 185, 142–154.

Foody, G.M., 2002. Status of land cover classification accuracy assessment. Remote Sens. Environ. 80, 185–201.

Gao, Z., Zhang, L., 2006. Multi-seasonal spectral characteristics analysis of coastal salt marsh vegetation in Shanghai, China. Estuar. Coast. Shelf Sci. 69, 217–224.

Ge, Z., Cao, H., Zhang, L., 2013. A process-based grid model for the simulation of range expansion of Spartina alterniflora on the coastal saltmarshes in the Yangtze estuary. Ecol. Eng. 58, 105–112.

Gong, P., Wang, J., Yu, L., Zhao, Y., Zhao, Y., Liang, L., Niu, Z., Huang, X., Fu, H., Liu, S., Li, C., Li, X., Fu, W., Liu, C., Xu, Y., Wang, X., Cheng, Q., Hu, L., Yao, W., Zhang, H., Zhu, P., Zhao, Z., Zhang, H., Zheng, Y., Ji, L., Zhang, Y., Chen, H., Yan, A., Guo, J., Yu, L., Wang, L., Liu, X., Shi, T., Zhu, M., Chen, Y., Yang, G., Tang, P., Xu, B., Giri, C., Clinton, N., Zhu, Z., Chen, J., Chen, J., 2012. Finer resolution observation and monitoring of global land cover: first mapping results with Landsat TM and ETM+ data. Int. J. Remote Sens. 34, 2607–2654.

Gorelick, N., Hancher, M., Dixon, M., Ilyushchenko, S., Thau, D., Moore, R., 2017. Google earth engine: planetary-scale geospatial analysis for everyone. Remote Sens. Environ. 202, 18–27.

Helman, D., Lensky, I., Tessler, N., Osem, Y., 2015. A phenology-based method for monitoring woody and herbaceous vegetation in mediterranean forests from NDVI time series. Remote Sens. 7, 12314–12335.

Herold, M., Mayaux, P., Woodcock, C.E., Baccini, A., Schmullius, C., 2008. Some challenges in global land cover mapping: an assessment of agreement and accuracy in existing 1 km datasets. Remote Sens. Environ. 112, 2538–2556.

Hladik, C., Schalles, J., Alber, M., 2013. Salt marsh elevation and habitat mapping using hyperspectral and LIDAR data. Remote Sens. Environ. 139, 318–330.

Hu, Z., Ge, Z., Ma, Q., Zhang, Z., Tang, C., Cao, H., Zhang, T., Li, B., Zhang, L., 2015. Revegetation of a native species in a newly formed tidal marsh under varying hydrological conditions and planting densities in the Yangtze estuary. Ecol. Eng. 83, 354–363.

Huang, H., 2009. A Research on Spatial-Temporal Dynamics of Saltmarsh Vegetation at the Intertidal Zone in Shanghai. East China Normal University, Shanghai.

Huang, H., Zhang, L., 2007a. Remote sensing analysis of range expansion of Spartina alterniflora at Jiuduansha shoals in Shanghai, China. J. Plant Ecol. 31, 75–82 (in Chinese).

Huang, H., Zhang, L., 2007b. A study of the population dynamics of Spartina alterniflora at Jiuduansha shoals, Shanghai, China. Ecol. Eng. 29, 164–172.

Huang, C., Goward, S.N., Masek, J.G., Thomas, N., Zhu, Z., Vogelmann, J.E., 2010. An automated approach for reconstructing recent forest disturbance history using dense Landsat time series stacks. Remote Sens. Environ. 114, 183–198.

Huete, A., Didan, K., Miura, T., Rodriguez, E.P., Gao, X., Ferreira, L.G., 2002. Overview of the radiometric and biophysical performance of the MODIS vegetation indices. Remote Sens. Environ. 83, 195–213.

Kennedy, R.E., Yang, Z., Cohen, W.B., 2010. Detecting trends in forest disturbance and recovery using yearly Landsat time series: 1. LandTrendr-Temporal segmentation algorithms. Remote Sens. Environ. 114, 2897–2910.

Kou, W., Xiao, X., Dong, J., Gan, S., Zhai, D., Zhang, G., Qin, Y., Li, L., 2015. Mapping deciduous rubber plantation areas and stand ages with PALSAR and Landsat images. Remote Sens. 7, 1048–1073.

Li, H., Zhang, L., Wang, D., 2006. Distribution of an exotic plant Spartina alterniflora in Shanghai. Biodivers. Sci. 14, 114.

Li, B., Liao, C., Zhang, X., Chen, H., Wang, Q., Chen, Z., Gan, X., Wu, J., Zhao, B., Ma, Z., Cheng, X., Jiang, L., Chen, J., 2009. Spartina alterniflora invasions in the Yangtze River estuary, China: an overview of current status and ecosystem effects. Ecol. Eng. 35, 511–520.

Lin, W., Chen, G., Guo, P., Zhu, W., Zhang, D., 2015. Remote-sensed monitoring of dominant plant species distribution and dynamics at Jiuduansha wetland in Shanghai, China. Remote Sens. 7, 10227–10241.

Lin, Y., Yu, J., Cai, J., Sneeuw, N., Li, F., 2018. Spatio-temporal analysis of wetland changes using a kernel extreme learning machine approach. Remote Sens. 10, 1129.

Liu, C., Jiang, H., Zhang, S., Li, C., Pan, X., Lu, J., Hou, Y., 2016. Expansion and management implications of invasive alien Spartina alterniflora in Yancheng salt marshes, China. Open J. Ecol 6, 113–128.

Liu, M., Li, H., Li, L., Man, W., Jia, M., Wang, Z., Lu, C., 2017. Monitoring the invasion of Spartina alterniflora using multi-source high-resolution imagery in the Zhangjiang estuary, China. Remote Sens. 9, 539.

Liu, M., Mao, D., Wang, Z., Li, L., Man, W., Jia, M., Ren, C., Zhang, Y., 2018. Rapid invasion of Spartina alterniflora in the coastal zone of mainland China: new observations from Landsat OLI images. Remote Sens. 10, 1933.

Lu, J., Zhang, Y., 2013. Spatial distribution of an invasive plant Spartina alterniflora and its potential as biofuels in China. Ecol. Eng. 52, 175–181.

Luo, M., 2019. Remote Sensing Monitoring and Ecosystem Service Value Assessment of Coastal Salt Marshes in China in 2015. Zhejiang University, Hangzhou.

Mao, D., Liu, M., Wang, Z., Li, L., Man, W., Jia, M., Zhang, Y., 2019. Rapid invasion of Spartina Alterniflora in the coastal zone of mainland China: spatiotemporal patterns and human prevention. Sensors 19, 2308.

Masek, J.G., Vermote, E.F., Saleous, N.E., Wolfe, R., Hall, F.G., Huemmrich, K.F., Gao, F., Kutler, J., Lim, T.K., 2006. A Landsat surface reflectance dataset for North America, 1990–2000. IEEE Geosci. Remote Sens. Lett. 3, 68–72.

Morris, J.T., Porter, D., Neet, M., Noble, P.A., Schmidt, L., Lapine, L., Jensen, J.R., 2005. Integrating LIDAR elevation data, multi-spectral imagery and neural network modelling for marsh characterization. Int. J. Remote Sens. 26, 5221–5234.

Olofsson, P., Foody, G.M., Stehman, S.V., Woodcock, C.E., 2013. Making better use of accuracy data in land change studies: estimating accuracy and area and quantifying uncertainty using stratified estimation. Remote Sens. Environ. 129, 122–131.

Olofsson, P., Foody, G.M., Herold, M., Stehman, S.V., Woodcock, C.E., Wulder, M.A., 2014. Good practices for estimating area and assessing accuracy of land change. Remote Sens. Environ. 148, 42–57.

Ouyang, Z., Gao, Y., Xie, X., Guo, H., Zhang, T., Zhao, B., 2013. Spectral discrimination of the invasive plant Spartina alterniflora at multiple phenological stages in a saltmarsh wetland. PLoS One 8, e67315.

Rosso, P.H., Ustin, S.L., Hastings, A., 2005. Mapping marshland vegetation of San Francisco Bay, California, using hyperspectral data. Int. J. Remote Sens. 26, 5169–5191.

Sun, Z., Gao, J., Zhao, R., 1992. Vegetation in the migratory bird natural reserve of the East Beach of Chongming Island. Shanghai Environ. Sci. 11, 22–25 (in Chinese).

Sun, C., Liu, Y., Zhao, S., Zhou, M., Yang, Y., Li, F., 2016. Classification mapping and species identification of salt marshes based on a short-time interval NDVI time-series from HJ-1 optical imagery. Int. J. Appl. Earth Obs. 45, 27–41.

Tang, C., 2016. Ecological control of Spartina alterniflora and improvement of birds habitats in Chongming Dongtan wetland, Shanghai. Wetland Sci. Manag. 12, 4–8 (in Chinese).

Tucker, C.J., 1979. Red and photographic infrared linear combinations fro monitoring vegetation. Remote Sens. Environ. 8, 127–150.

van Beijma, S., Comber, A., Lamb, A., 2014. Random forest classification of salt marsh vegetation habitats using quad-polarimetric airborne SAR, elevation and optical RS data. Remote Sens. Environ. 149, 118–129.

Vaz, A.S., Alcaraz-Segura, D., Campos, J.C., Vicente, J.R., Honrado, J.P., 2018. Managing plant invasions through the lens of remote sensing: a review of progress and the way forward. Sci. Total Environ. 642, 1328–1339.

Vermote, E., Justice, C., Claverie, M., Franch, B., 2016. Preliminary analysis of the performance of the Landsat 8/OLI land surface reflectance product. Remote Sens. Environ. 185, 46–56.

Wan, H., Wang, Q., Jiang, D., Fu, J., Yang, Y., Liu, X., 2014. Monitoring the invasion of Spartina alterniflora using very high resolution unmanned aerial vehicle imagery in Beihai, Guangxi (China). Sci. World J. 2014, 7.

Wang, Q., 2007. The Dynamics of Plant Community Distribution of the Salt Marshes in the Yangtze River Estuary as Influenced by *Spartina alterniflora* Invasions. Fudan University, Shanghai.

Wang, Q., 2011. Spartina alterniflora invasion in Chongming Dongtan, Shanghai: history, status and prediction. Resour. Environ. Yangtze Basin 20, 690–696 (in Chinese).

Wang, A., Chen, J., Jing, C., Ye, G., Wu, J., Huang, Z., Zhou, C., 2015. Monitoring the invasion of Spartina alterniflora from 1993 to 2014 with Landsat TM and SPOT 6 satellite data in Yueqing Bay, China. PLoS One 10, e0135538.

Wang, J., Xiao, X., Qin, Y., Dong, J., Geissler, G., Zhang, G., Cejda, N., Alikhani, B., Doughty, R.B., 2017. Mapping the dynamics of eastern redcedar encroachment into grasslands during 1984-2010 through PALSAR and time series Landsat images. Remote Sens. Environ. 190, 233–246.

Wang, X., Xiao, X., Zou, Z., Chen, B., Ma, J., Dong, J., Doughty, R.B., Zhong, Q., Qin, Y., Dai, S., Li, X., Zhao, B., Li, B., 2018. Tracking annual changes of coastal tidal flats in China during 1986–2016 through analyses of Landsat images with Google earth engine. Remote Sens. Environ. 238, 110987.

Wang, X., Xiao, X., Zou, Z., Hou, L., Qin, Y., Dong, J., Doughty, R.B., Chen, B., Zhang, X., Chen, Y., Ma, J., Zhao, B., Li, B., 2020. Mapping coastal wetlands of China using time series Landsat images in 2018 and Google earth engine. ISPRS J. Photogramm. Remote Sens. 163, 312–326.

Wu, C., Peng, D., Soudani, K., Siebicke, L., Gough, C.M., Arain, M.A., Bohrer, G., Lafleur, P.M., Peichl, M., Gonsamo, A., Xu, S., Fang, B., Ge, Q., 2017. Land surface phenology derived from normalized difference vegetation index (NDVI) at global FLUXNET sites. Agric. For. Meteorol. 233, 171–182.

Wu, Y., Xiao, X., Chen, B., Ma, J., Wang, X., Zhang, Y., Zhao, B., Li, B., 2018. Tracking the phenology and expansion of Spartina alterniflora coastal wetland by time series MODIS and Landsat images. Multimed. Tools Appl. 79, 5175–5195.

Wulder, M.A., White, J.C., Loveland, T.R., Woodcock, C.E., Belward, A.S., Cohen, W.B., Fosnight, E.A., Shaw, J., Masek, J.G., Roy, D.P., 2016. The global Landsat archive: status, consolidation, and direction. Remote Sens. Environ. 185, 271–283.
Wulder, M.A., Loveland, T.R., Roy, D.P., Crawford, C.J., Masek, J.G., Woodcock, C.E., Allen, R.G., Anderson, M.C., Belward, A.S., Cohen, W.B., Dwyer, J., Erb, A., Gao, F., Griffiths, P., Helder, D., Hermosilla, T., Hipple, J.D., Hostert, P., Hughes, M.J., Huntington, J., Johnson, D.M., Kennedy, R., Kilic, A., Li, Z., Lymburner, L., McCorkel, J., Pahlevan, N., Scambos, T.A., Schaaf, C., Schott, J.R., Sheng, Y., Storey, J., Vermote, E., Vogelmann, J., White, J.C., Wynne, R.H., Zhu, Z., 2019. Current status of Landsat program, science, and applications. Remote Sens. Environ. 225, 127–147.
Xiao, X., Boles, S., Liu, J., Zhuang, D., Frolking, S., Li, C., Salas, W., Moore, B., 2005. Mapping paddy rice agriculture in southern China using multi-temporal MODIS images. Remote Sens. Environ. 95, 480–492.
Xiao, X., Boles, S., Frolking, S., Li, C., Babu, J.Y., Salas, W., Moore, B., 2006. Mapping paddy rice agriculture in south and Southeast Asia using multi-temporal MODIS images. Remote Sens. Environ. 100, 95–113.
Xiao, X., Biradar, C., Czarnecki, C., Alabi, T., Keller, M., 2009. A simple algorithm for large-scale mapping of evergreen forests in tropical America, Africa and Asia. Remote Sens. 1, 355–374.
Xiao, D., Zhang, L., Zhu, Z., 2010. The range expansion patterns of Spartina alterniflora on salt marshes in the Yangtze Estuary, China. Estuar. Coast. Shelf Sci. 88, 99–104.
Zhang, X., Friedl, M.A., Schaaf, C.B., Strahler, A.H., Hodges, J.C.F., Gao, F., Reed, B.C., Huete, A., 2003. Monitoring vegetation phenology using MODIS. Remote Sens. Environ. 84, 471–475.
Zhang, R., Shen, Y., Lu, L., Yan, S., Wang, Y., Li, J., Zhang, Z., 2004. Formation of Spartina alterniflora salt marshes on the coast of Jiangsu Province, Spain. Ecol. Eng. 23, 95–105.
Zhang, X., Friedl, M.A., Schaaf, C.B., 2006. Global vegetation phenology from moderate resolution imaging Spectroradiometer (MODIS): evaluation of global patterns and comparison with in situ measurements. J. Geophys. Res. Biogeosci. 111.
Zhang, G., Xiao, X., Dong, J., Kou, W., Jin, C., Qin, Y., Zhou, Y., Wang, J., Menarguez, M.A., Biradar, C., 2015. Mapping paddy rice planting areas through time series analysis of MODIS land surface temperature and vegetation index data. ISPRS J. Photogramm. Remote Sens. 106, 157–171.
Zhang, D., Hu, Y., Liu, M., Chang, Y., Yan, X., Bu, R., Zhao, D., Li, Z., 2017. Introduction and spread of an exotic plant, Spartina alterniflora, along coastal marshes of China. Wetlands 37, 1181–1193.
Zhu, Z., Woodcock, C.E., 2012. Object-based cloud and cloud shadow detection in Landsat imagery. Remote Sens. Environ. 118, 83–94.
Zhu, C., Zhang, X., Qi, J., 2016. Detecting and assessing Spartina invasion in coastal region of China: a case study in the Xiangshan Bay. Acta Oceanol. Sin. 35, 35–43.
Zou, Z., Dong, J., Menarguez, M.A., Xiao, X., Qin, Y., Doughty, R.B., Hooker, K.V., Hambright, K.D., 2017. Continued decrease of open surface water body area in Oklahoma during 1984-2015. Sci. Total Environ. 595, 451–460.
Zou, Z., Xiao, X., Dong, J., Qin, Y., Doughty, R.B., Menarguez, M.A., Zhang, G., Wang, J., 2018. Divergent trends of open-surface water body area in the contiguous United States from 1984 to 2016. Proc. Natl. Acad. Sci. U. S. A. 115, 3810–3815.
Zuo, P., Zhao, S., Liu, C.a., Wang, C., Liang, Y., 2012. Distribution of Spartina spp. along China's coast. Ecol. Eng. 40, 160–166.